SPATIALLY-SEPARATED ATOMIC LAYER DEPOSITION OF Al_2O_3, A NEW OPTION FOR HIGH-THROUGHPUT Si SOLAR CELL PASSIVATION

B. Vermang[1,2], F. Werner[3], W. Stals[4], A. Lorenz[1], A. Rothschild[1], J. John[1],
J. Poortmans[1,2], R. Mertens[1,2], R. Gortzen[4], F. Roozeboom[5], and J. Schmidt[3,6]
[1]Imec, Kapeldreef 75, 3001 Leuven, Belgium
[2]Katholieke Universiteit Leuven (K.U.Leuven), Oude Markt 13 Bus 5005, 3000 Leuven, Belgium
[3]Institute for Solar Energy Research Hamelin (ISFH), Am Ohrberg 1, 31860 Emmerthal, Germany
[4]SoLayTec, Dillenburgstraat 9G, 5652 AM Eindhoven, The Netherlands
[5]Eindhoven University of Technology (TU/e), PO Box 513, 5600 MB Eindhoven, The Netherlands
[6]Institute of Solid-State Physics (University of Hanover), Appelstrasse 2, 30167 Hannover, Germany

ABSTRACT

A next generation material for surface passivation of crystalline Si is atomic layer deposited (ALD) Al_2O_3. However, conventional time-resolved ALD is limited by its low deposition rate.

Initially, an experimental high-deposition-rate prototype ALD reactor based on the spatially-separated ALD principle has been developed and Al_2O_3 deposition rates up to 1.2 nm/s have been demonstrated. Later, the spatial ALD technique has been transferred to an actual in-line process development tool for commercial high-throughput ALD of Al_2O_3, resulting in a deposition rate of 4 monolayers per second, or ~30 nm/min.

The passivation quality and uniformity of the spatially-separated ALD Al_2O_3 films are evaluated on CZ p-type and CZ and FZ n-type Si, applying quasi-steady-state photo-conductance (QSSPC), carrier density imaging (CDI) and infrared lifetime mapping (ILM). In all cases, a spatial ALD Al_2O_3 layer of only 10 nm reached an excellent passivation quality and uniformity, comparable to reference wafers passivated by equivalent temporal plasma-assisted (PA) or thermal ALD Al_2O_3. Effective surface recombination velocities as low as 1.1 or 2.9 cm/s were obtained after annealing at 350 °C or firing, respectively.

Using spatial ALD Al_2O_3 passivated local Al BSF p-type Si solar cells, the sufficient passivation of this high-throughput Al_2O_3 layer is evaluated: an average gain in Voc as compared to SiO_x rear passivated i-PERC cells is obtained

INTRODUCTION

Passivation of c-Si solar cells is key for the development of high-efficiency solar cells. It has been shown that atomic layer deposition (ALD) of Al_2O_3 provides an adequate level of surface passivation for both p-type and n-type substrates: high-efficiency and industrial type solar cells comprising lab-scale ALD Al_2O_3 passivation layers have already been demonstrated ([1] and references herein). The underlying mechanism is based on chemical [1,2] and field-effect passivation [3].

However, conventional time-resolved ALD is limited by its low deposition rate. In the temporal mode the deposition reaction is divided in two time-sequenced self-limiting half-reactions, both being separated by a purge step to desorb precursors from the surface areas where the reaction has reached completion ([4] and [5]). It is clear that a faster and cost-effective ALD concept is needed to meet the throughput demands of the PV market.
Instead of temporal separation, the ultra-fast ALD concept is based on the spatial separation of the half-reactions ([6], and references therein): such reactor has separate zones exposing the precursors one by one to a substrate that rotates, reciprocates or travels linearly underneath an array of different precursor injectors. The reactor used in this study operates at atmospheric pressure by using gas bearings between the zones as excellent cross-diffusion barriers. Thus spatially-separated ALD makes purge steps obsolete and brings half-reaction timescales down to a few milliseconds. In this way very high deposition rates are achieved, while maintaining the required high film quality.

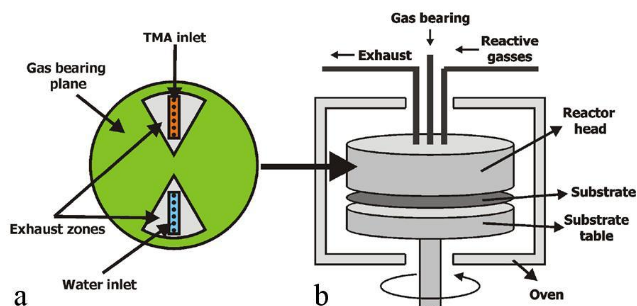

Figure 1 (a) Schematic drawing of the bottom side of the experimental spatial ALD reactor head, where the trimethyl-aluminium (TMA) and water half-reaction zones are integrated into inlets surrounded by exhaust zones and gas bearing planes; (b) Schematic drawing of the reactor.

First, as sketched in Fig.1 an experimental high-speed prototype ALD reactor has been developed [7], giving deposition rates up to 1.2 nm/s - growth per cycles (GPC) of 1.2 Å/cycle - and excellent thickness and refractive index uniformities. With the experimental set-up, a 3 cm wide ring-shaped track of Al_2O_3 has been deposited,

corresponding to the width and position of the deposition inlets.

Later, the spatial ALD technique has been transferred to an in-line process development tool (PDT) manufactured by SoLayTec. As depicted in Fig. 2: in the PDT the wafer is heated to 200 °C in 6 s, after which it is cycled through the core reactor at a rate of 2 Hz, resulting in a deposition rate of 4 monolayers per second, or ~30 nm/min.

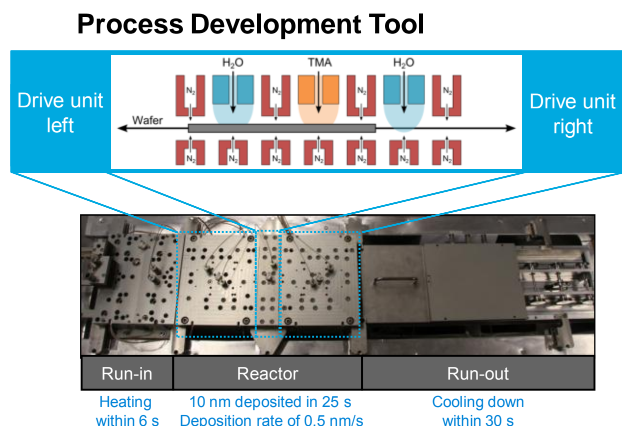

Figure 2 Picture of the in-line process development tool: wafers are heated to 200 °C in 6 s, after which they are cycled through the core reactor where the TMA and water half-reaction zones are separated by nitrogen curtains. Contactless transport of the wafer is facilitated by nitrogen gas bearings below the wafer.

In this work, the passivation properties of spatially-separated ALD Al_2O_3 films deposited by the experimental and the PDT tool are assessed via lifetime devices, employing quasi-steady-state photo-conductance (QSSPC), carrier density imaging (CDI) and infrared lifetime mapping (ILM). Also Al_2O_3 / SiN_x passivated local Al back surface field (BSF) p-type Si solar cells have been fabricated to evaluate the passivation at cell level.

EXPERIMENTAL

Float-Zone (FZ) and Czochralski (CZ) grown, p-type as well as n-type Si (100) wafers were used to assess the surface passivation properties as general as possible: (i) 120 µm thick p-type CZ Si wafers of 2 Ω.cm, (ii) 180 µm thick n-type CZ Si wafers of 4 Ω.cm or (iii) 250 µm thick mirror-polished n-type FZ Si wafers of 2.4 Ω.cm. The wafer types are specified in the text.

Si wafer cleanings have an HF-last or oxidizing last step and finish with Marangoni drying, more details can be found in [2] and are refined in the text if essential.

The reference temporal thermal or plasma-assisted (PA-) ALD Al_2O_3 films were grown in commercial reactors: a Savannah S200 from Cambridge Nanotech or an Oxford FlexAL™ reactor, respectively, and underwent a post-deposition annealing as specified in the text.

In order to apply QSSPC, CDI or ILM, all samples were passivated on both sides. QSSPC is used to quantify the surface passivation level by measuring the effective lifetime (τ_{eff}). It is measured by a lifetime tester (Sinton WCT-100) in the generalized or transient approach. In a first approximation τ_{eff} of a symmetrically passivated c-Si wafer can be written as in Eq. (1),

$$\frac{1}{\tau_{eff}} = \frac{1}{\tau_{bulk}} + \frac{2S_{eff}}{W} \quad (1)$$

with τ_{bulk} the bulk lifetime, W the c-Si wafer thickness and S_{eff} the effective surface recombination velocity (SRV) [8].

In the dynamic ILM analysis, wafers are exposed to a constant illumination intensity, which has to be carefully set to compare lifetime mappings of different wafers at a similar injection density (Δn). The CDI technique is a further development of ILM. In this study, CDI and ILM are used to qualify the passivation uniformity and quantity [9].

The used current-voltage (IV) setup is a steady-state Xe lamp solar simulator (Wacom Electric Co., WXS-200S-20, AM 1.5G) with an illuminated area of 200 x 200 mm^2, a small bias error and a good stability over time, as shown in [10].

RESULTS AND DISCUSSION

(1) Experimental prototype reactor ALD Al_2O_3 surface passivation of p-type CZ Si

Spatially-separated ALD Al_2O_3 layers with nominal thicknesses of 5, 10 and 30 nm have been deposited on p-type CZ Si material. This is done in the experimental rotary spatial ALD reactor, at rotation frequencies of 60, 120 or 300 rpm using a partial H_2O pressure of 124 or 340 mbar. Also conventional temporal ALD Al_2O_3 films of equivalent thicknesses were deposited on identical wafers. After deposition, each wafer was diced in 4 pieces and received one of the following thermal treatments: (i) 20 minutes in forming gas (FG) at 350 °C, (ii) 20 minutes in N_2 at 350 °C, (iii) 30 minutes in FG at 350 °C or, (iv) 30 minutes in FG at 450 °C.

Since saw damage removed p-type CZ Si of only 120 µm material is used to characterize the surface passivation, an estimation of the τ_{bulk} is needed. This is done using temporal ALD Al_2O_3 - a passivation process that leads to surface recombination velocities well below 2 cm/s [1] - to passivate wafers of various thicknesses of equivalent CZ Si material (starting thickness is 700 um and used etching solution is NaOH:H_2O). Fig. 3 shows a plot of the inverse effective lifetime as a function of the inverse wafer thickness. Using Eq. 1 one can derive an estimation of τ_{bulk}, which is the intercept of the linear fit with the vertical axis. This estimation of τ_{bulk} is used to calculate S_{eff} for the best passivating 5, 10 and 30 nm thick spatial and temporal ALD Al_2O_3 layers after annealing, see Fig. 4. It is apparent that spatial ALD Al_2O_3 films of increasing thickness provide an increasing surface passivation level. Moreover, on p-type CZ Si, 10 and 30 nm thick spatial ALD Al_2O_3 layers can achieve the same level of surface passivation as equivalent temporal ALD Al_2O_3 layers.

However, this is not the case for a thin spatial ALD Al_2O_3 layer: the final passivation level of a 5 nm spatially deposited layer is influenced by the rotation speed or H_2O flow used; this is shown more clearly on n-type FZ Si.

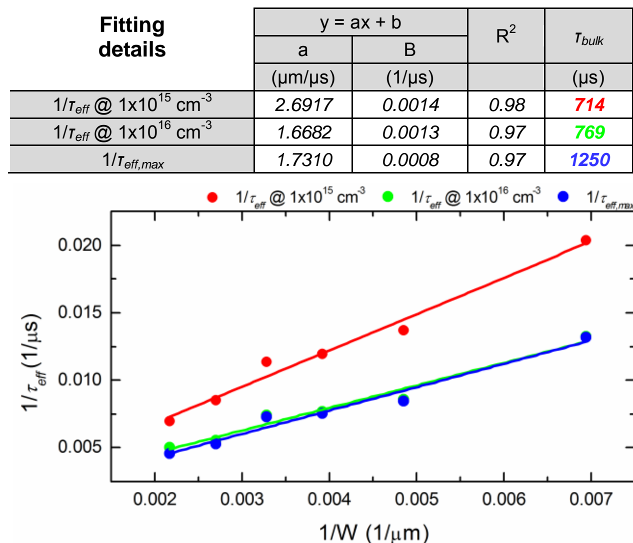

Fitting details	y = ax + b		R^2	τ_{bulk}
	a	B		
	(µm/µs)	(1/µs)		(µs)
$1/\tau_{eff}$ @ 1×10^{15} cm^{-3}	2.6917	0.0014	0.98	714
$1/\tau_{eff}$ @ 1×10^{16} cm^{-3}	1.6682	0.0013	0.97	769
$1/\tau_{eff,max}$	1.7310	0.0008	0.97	1250

Figure 3 Inverse effective lifetime as a function of inverse wafer thickness for the same material and the same surface passivation: respectively 2 Ω.cm p-type CZ Si and 30 nm of temporal ALD Al_2O_3, forming gas annealed at 350 °C for 30 minutes. Also the details of the linear fits are given.

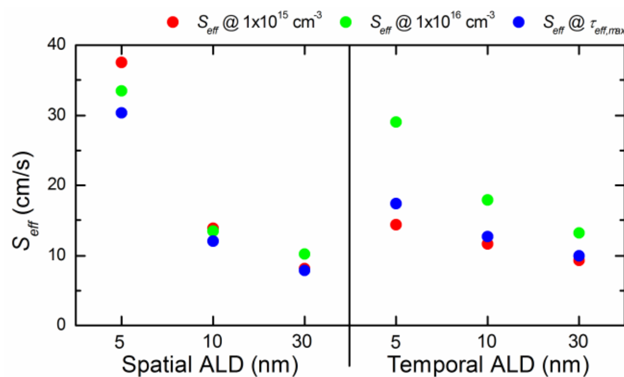

Figure 4 Effective surface recombination velocities of spatially-separated and conventional temporal ALD Al_2O_3 of equivalent thickness, both deposited at 200 °C on both sides of a 120 µm thick p-type CZ Si substrate of 2 Ω.cm. All samples received the most favorable annealing (N_2 or FG, 350 or 450 °C, and 20 or 30 min), which leads to the best surface passivation.

(2) Experimental prototype reactor ALD Al_2O_3 surface passivation of n-type FZ Si

A similar experimental matrix was completed on high-quality and mirror polished n-type FZ material: Al_2O_3 layers with nominal thicknesses of 5, 10 and 30 nm have been deposited in the spatial ALD reactor, at rotational frequencies of 2, 5 or 10 Hz using a partial H_2O pressure of 62, 124 or 340 mbar and a deposition temperature of 200 °C. Also conventional temporal ALD Al_2O_3 films of equivalent thicknesses have been deposited on identical wafers.

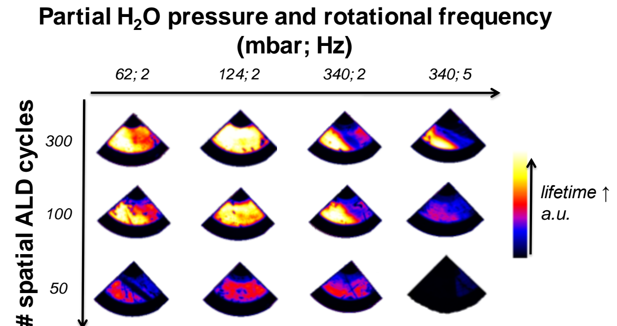

Figure 5 Carrier density images of n-type FZ Si passivated with spatial ALD Al_2O_3, measured after annealing at 350 °C in N_2. The sample size is ¼ of a 150 mm round wafer and the scale is in arbitrary units.

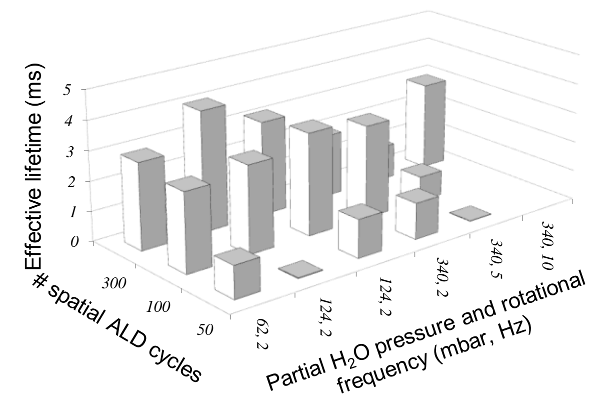

Figure 6 Effective lifetimes at 1×10^{15} cm^{-3} excess carrier density measured after annealing at 350 °C in N_2 within the ring-shaped spatially-separated ALD Al_2O_3 passivation layers deposited on n-type FZ Si.

CDI images (Fig. 5) clearly show that for samples with only 5 nm Al_2O_3 films the spatial ALD growth mechanism does not give a uniform end result and, hence, low passivation quality. They also prove that a rotational frequency of 2 Hz and a partial H_2O pressure of 124 mbar are the most suited for the spatial ALD tool. For the samples with 10 and 30 nm of spatial ALD Al_2O_3 films, it is clear that lower or higher H_2O flows as well as higher rotation speeds lead to lower passivation quality and uniformity. As shown in Fig. 6, QSSPC measurements at 1×10^{15} cm^{-3} excess carrier density are in very good agreement with these CDI images. The experimental matrix contains also 2 wafers coated with 5, 10 or 30 nm of spatially-separated ALD Al_2O_3 using this most favorable H_2O pressure and rotational frequency to check the reproducibility of the results.

Important to mention is that after a thermal treatment which mimics the firing step in solar cell processing ([11]) 30 nm of spatially-separated ALD Al_2O_3 on 250 μm thick n-type FZ Si wafers of 2.4 Ω.cm did lead to effective surface recombination velocities as low as 2.9 cm/s, compared to 1.9 cm/s in the case of 30 nm of temporal ALD Al_2O_3.

(3) In-line process development tool ALD Al_2O_3 surface passivation of n-type CZ Si

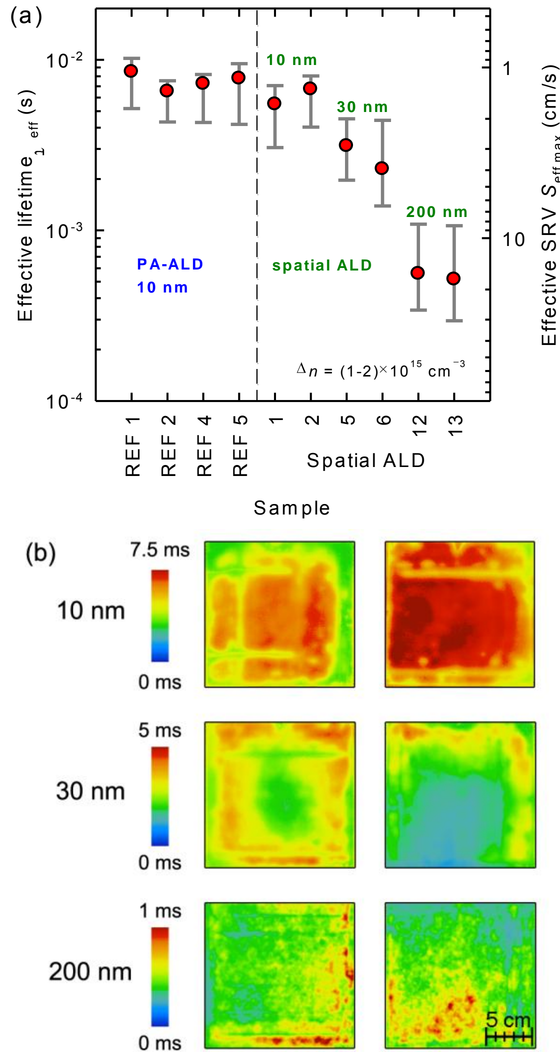

Figure 7 (a) Effective lifetime τ_{eff} and maximum effective SRV $S_{eff,max}$ for Al_2O_3 thicknesses of 10, 30, and 200 nm deposited by spatial ALD, and 10 nm deposited by plasma-assisted ALD, respectively. The lifetime is calculated from the lifetime mappings shown in (b) by averaging over the wafer area, error bars denote the minimum and maximum values; (b) Spatially resolved lifetime mappings measured by dynamic ILM for 15.6x15.6 cm^2 n-type CZ Si wafers passivated by spatial ALD Al_2O_3 [13].

Al_2O_3 films with a thickness of 10, 30 and 200 nm, respectively, were deposited by spatial ALD on 4 Ω.cm n-type CZ Si wafers with a size of 15.6×15.6 cm² (full-square) and a thickness of 180 μm. The samples were subsequently annealed at 350 °C for 30 min in N_2 ambient to optimize the passivation. In addition, four wafers were passivated with 10 nm of Al_2O_3 deposited by PA-ALD and annealed at 425 °C for 15 min. These wafers serve as a reference, as Al_2O_3 deposited by PA-ALD is known to yield extremely low surface recombination velocities on lowly doped n-type silicon [12].

Fig. 7(a) shows the effective lifetime τ_{eff} measured by dynamic ILM and averaged over the wafer area, excluding ~0.5 cm around the wafer edges. Since the substrate is lowly doped n-type Si, τ_{bulk} was assumed infinite in Eq. (1). The error bars denote the minimum and maximum lifetime values recorded within this area. The spatially resolved lifetime mappings in Fig. 7(b) correspond to the data points shown in Fig. 7(a) for the samples passivated by spatial ALD. The reference wafers passivated by PA-ALD yield effective lifetimes at a mean injection density of Δn = (1–2)×10^{15} cm^{-3} between 4.2 and 10.2 ms, corresponding to a maximum effective SRV or $S_{eff,max}$ = 0.9 – 2.2 cm/s. A comparable level of surface passivation is achieved with 10 nm of Al_2O_3 deposited by high-rate spatial ALD, yielding effective lifetimes between 3.1 and 8.1 ms ($S_{eff,max}$ = 1.1 – 2.9 cm/s). A slight degradation of the effective lifetime along two parallel stripes is attributed to the wafer handling prior to or during deposition, hence adjustments to the wafer handling promise further improvements to the already excellent surface passivation quality.

A reduced effective lifetime is observed for a spatial Al_2O_3 thickness exceeding 10 nm. For a film thickness of 30 nm this effect is marginal, yielding effective lifetimes between 1.4 and 4.5 ms ($S_{eff,max}$ = 2.0 – 6.5 cm/s). For a film thickness of 200 nm, however, significantly reduced effective lifetimes between 300 μs and 1.1 ms are measured, corresponding to $S_{eff,max}$ = 8.2 – 30.5 cm/s. The reduced lifetime for thick Al_2O_3 layers is of no concern for the industrial fabrication of solar cells, as such thick layers of Al_2O_3 are usually not desired.

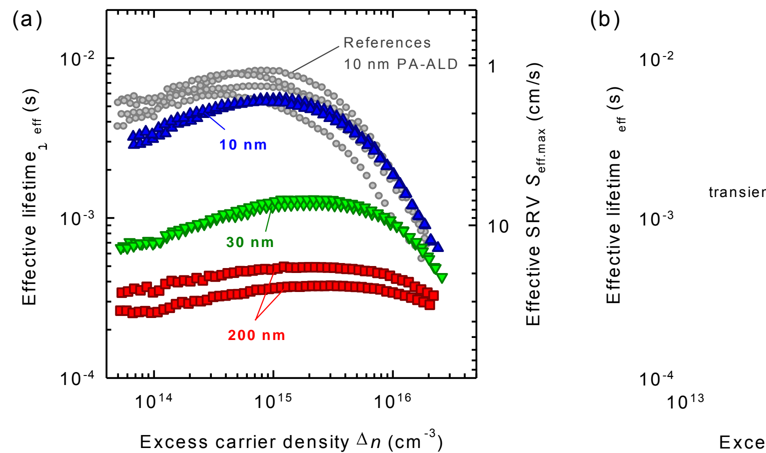

Figure 8 Effective lifetime τ_{eff} and maximum effective SRV $S_{eff,max}$ as function of injection density Δn measured by transient QSSPC. The Al_2O_3 thickness is

10, 30, and 200 nm deposited by spatial ALD, and 10 nm deposited by plasma-assisted ALD, respectively [13].

The dependence of the surface passivation quality on injection density is addressed in Fig. 8, it shows the effective lifetime τ_{eff} and maximum effective SRV $S_{eff,max}$ as a function of Δn measured by transient QSSPC. In agreement with Fig. 7 the reference samples passivated by PA-ALD and the samples passivated with 10 nm Al_2O_3 deposited by spatial ALD show an excellent level of surface passivation. For thicker Al_2O_3 layers the effective lifetime is reduced. Independent of the Al_2O_3 thickness all samples only show a minor injection density dependence of the effective lifetime [13].

(4) In-line process development tool ALD Al_2O_3 rear surface passivation of local Al back surface field (BSF) p-type Si solar cells

Rear surface passivation of local Al BSF Si solar cells by Al_2O_3 only is not possible, a capping layer as barrier during the co-firing process step (equals a rapid thermal processing with a peak temperature of 835 °C for 1-2 s, see [11]) is needed. In this work plasma-enhanced chemical vapour deposition (PECVD) SiN_x is used as capping for Al_2O_3 rear surface passivation.
However, a remaining fundamental concern is blistering (see Fig. 9) in Al_2O_3 layers: blistering is the partial de-lamination of a thick enough Al_2O_3 layer caused by gaseous desorption in the Al_2O_3 layer upon thermal treatments above a critical temperature: the Al_2O_3 layer acts as a gas barrier and bubble formation occurs [14,15]. Capping Al_2O_3 with other dielectrics makes the situation more complicated. For example: capping Al_2O_3 with PECVD SiN_x deposited at a temperature above 400 °C means that the critical temperature for gaseous desorption is reached and the Al_2O_3 / SiN_x stack is an even more effective gas barrier, therefore blistering is very likely to occur. Using a thin enough Al_2O_3 layer and performing an annealing step prior to SiN_x capping is the solution: the Al_2O_3 is out-gassed prior to SiN_x capping and can still have adequate passivation properties as shown in [14].

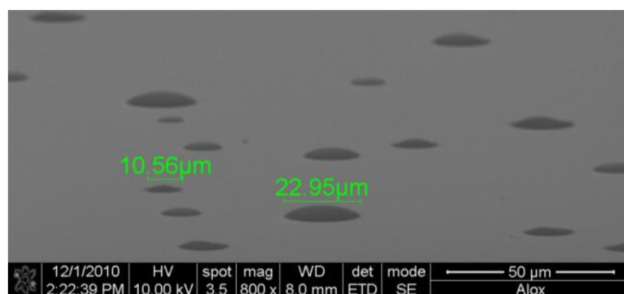

Figure 9 SEM tilted top-view of a blistered ALD Al_2O_3 layer on a mirror-polished c-Si substrate.

Al_2O_3 passivated local Al BSF and reference industrial passivated emitter and rear cell-type (i-PERC, see [16] and references herein) Si solar cells are made, see table I for the process sequences. In the case of the Al_2O_3 passivated Al BSF cells, thin ALD Al_2O_3 layers (5 to 10 nm) and 600 °C as out-gassing temperature have been used.

Table I: Baseline Al_2O_3 passivated local Al BSF solar cell (left) and i-PERC (right) process sequences.

Al_2O_3 passivated local Al BSF p-type Si solar cells	*i-PERC*
Texturing front and polishing rear	
Diffusion ($POCl_3$) front	
ALD Al_2O_3 passivation rear	LQCVD SiO_x passivation rear
Out-gassing	
PECVD SiN_x capping rear	
Anti reflection coating (SiN_x) front	
Local point contact laser ablation of the rear dielectric	
Al sputtering rear and Ag screen-printing front	
Co-firing	

As shown in Fig. 10, the average Voc of spatial ALD Al_2O_3 passivated local Al BSF Si cells is clearly enhanced as a function of out-gassing temperature due to the reduction of blistering (confirmed by optical microscopy). Even more, an average gain in Voc as compared to the SiO_x rear passivated i-PERC reference cells is shown. It has to be noted that due to some minor issues with the PDT injector head, the Si wafers were not completely deposited by Al_2O_3 for the out-gassed cells (a track of 1x12.5 cm^2 was missing). Therefore, the eventual gain in Voc compared to SiO_x passivated local Al BSF cells is expected to be in the range of at least 5.1 mV as already observed for temporal ALD Al_2O_3 passivated cells [14].

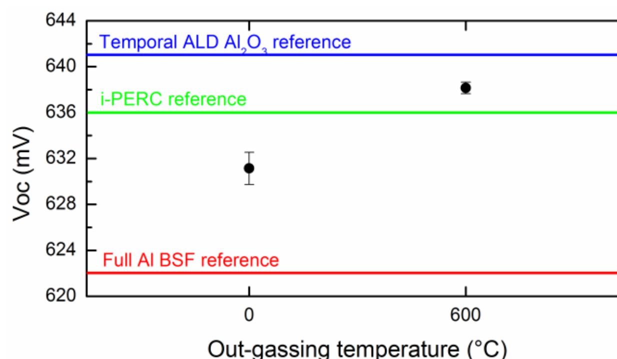

Figure 10 Average Voc of spatial ALD Al_2O_3 passivated local Al BSF Si cells as a function of out-gassing temperature, where the out-gassing is performed in between the Al_2O_3 deposition and SiN_x capping. Also for (i) full Al BSF, (ii) i-PERC and (iii) temporal ALD Al_2O_3 passivated local Al BSF reference cells the achieved average Voc is indicated.

In the case of the spatial Al_2O_3 passivated local Al BSF cells out-gassed at 600 °C, a best cell conversion efficiency of 18.0 % is found. This compared to 18.5 % for the SiO_x rear passivated i-PERC reference. There is an obvious gain in open circuit voltage Voc of 2 mV, nevertheless also a clear decrease in short circuit current Jsc of 0.9 mA/cm^2. See table II for all cell characterization results.

Table II: Overview of the cell characterization results (AM 1.5G) for the 148.25 cm^2 i-PERC and spatial ALD Al_2O_3 passivated local Al BSF Si solar cells. The process sequences are given in table I. The cells are 150 µm thick, have a base resistivity of 2 Ω.cm and an emitter of 60 Ω/sq.

Cell type		Jsc (mA/cm^2)	Voc (mV)	FF (%)	Eta (%)
i-PERC reference	Avg. (4 cells)	37.1 ± 0.1	636.1 ± 1.2	77.7 ± 0.6	18.4 ± 0.2
	Best cell	*37.1*	*636.8*	*78.2*	*18.5*
Al_2O_3 pass. local Al BSF cells	Avg. (4 cells)	36.2 ± 0.1	638.1 ± 0.5	77.4 ± 0.5	17.9 ± 0.1
	Best cell	*36.1*	*638.4*	*77.8*	*18.0*

It is demonstrated that the spatial ALD Al_2O_3 passivated local Al BSF cells show an enhanced rear surface passivition but lower back reflection compared to the SiO_x passivated i-PERC cells. From internal quantum efficiency (IQE) measurements, it is clear that the Al_2O_3 passivated cells show (i) no bias light dependency of the Jsc, and (ii) a lower SRV_{rear} (estimated via PC1D fitting of the IQE curves). The fact, that Al_2O_3 passivated cells are not bias light dependent confirms the expected lack of a shunted inversion layer due to the presence of fixed negative charges in the Al_2O_3 dielectric layer [3] and the lower SRV_{rear} is reflected in higher Voc's. However, reflectance measurements from 1000 to 1200 nm demonstrate that the rear reflectance is lower for all Al_2O_3 / SiN_x rear passivation stacks, which is also revealed in lower Jsc's.

CONCLUSIONS

First, an experimental high-speed prototype ALD reactor has been developed [7], giving deposition rates up to 1.2 nm/s and excellent thickness and refractive index uniformities. Later, the spatial ALD technique has been transferred to an in-line process development tool manufactured by SoLayTec.

For both tools, the surface passivation of spatial ALD Al_2O_3 layer is assessed via QSSPC, CDI and ILM lifetime measurements on various wafer types: (i) 120 µm thick p-type CZ Si wafers of 2 Ω.cm, (ii) 180 µm thick n-type CZ Si wafers of 4 Ω.cm or (iii) 250 µm thick mirror-polished n-type FZ Si wafers of 2.4 Ω.cm. In all cases, a spatial ALD Al_2O_3 layer of only 10 nm reached an excellent passivation quality and uniformity comparable to reference wafers passivated by equivalent temporal plasma-assisted (PA) or thermal ALD Al_2O_3. Passivating n-type Si wafers, surface recombination velocities as low as 1.1 or 2.9 cm/s were obtained after annealing at 350 °C or firing, respectively.

Using spatial ALD Al_2O_3 passivated local Al BSF p-type Si solar cells, the sufficient passivation of this high-throughput Al_2O_3 layer is evaluated: an average gain in Voc as compared to SiO_x rear passivated i-PERC cells is shown.

REFERENCES

[1] B. Vermang et al., "Spatially-separated Atomic Layer Deposition of Al_2O_3, a New Option for High-throughput Si Solar Cell Passivation", *Prog. Photovolt: Res. Appl.*, in press (DOI: 10.1002/pip.1092).

[2] B. Vermang et al., "Surface Passivation for Si Solar Cells: a Combination of Advanced Surface Cleaning and Thermal Atomic Layer Deposition of Al_2O_3", *Proc. 25th EU PVSEC and 5th WC PEC*, 2010, pp. 1118-1120.

[3] A. Rothschild et al., "ALD-Al_2O_3 Passivation for Solar Cells: Charge Investigation", *Proc. 25th EU PVSEC and 5th WC PEC*, 2010, pp. 1382-1385.

[4] R. L. Puurunen, "Surface Chemistry of Atomic Layer Deposition: A Case Study for the Trimethylaluminum / Water Process", *J. Appl. Phys.* **97**, 2005, 121301.

[5] S. M. George, "Atomic Layer Deposition: An Overview", *Chem. Rev.* **110**, 2010, pp.111–131.

[6] D. H. Levy et al., "Oxide Electronics by Spatial Atomic Layer Deposition", *J. Display Technol.* **5**, 2009, pp. 484.

[7] P. Poodt et al., "Ultra Fast Atomic Layer Deposition of Aluminum Oxide Layers for Solar Cell Passivation", *Adv. Mater.* **22**, 2010, pp. 3564–3567.

[8] M. J. Kerr et al., "Very Low Bulk and Surface Recombination in Oxidized Silicon Wafers", *Semicond. Sci. Technol.* **17**, 2002, pp.35-38.

[9] J. Isenberg et al., "Imaging Method for Laterally Resolved Measurement of Minority Carrier Densities and Lifetimes: Measurement Principle and First Applications", *J. Appl. Phys.* **93**, 2003, pp. 4268-4275.

[10] M. Debucquoy et al., "Optimization of the IV Measurement of Advanced Structures", *Proc. 25th EU PVSEC and 5th WC PEC*, 2010, pp. 381-384.

[11] F. Huster et al., "Investigation of the Alloying Process of Screen Printed Aluminium Pastes for the BSF Formation on Silicon Solar Cells", *Proc. 20th EU PVSEC*, 2005, pp. 1466-1469.

[12] B. Hoex et al., "Ultralow Surface Recombination of c-Si Substrates Passivated by Plasma-Assisted Atomic Layer Deposited Al_2O_3", *Appl. Phys. Lett.* **89**, 2006, pp. 042112.

[13] F. Werner et al., "High-rate Atomic Layer Deposition of Al_2O_3 for the Surface Passivation of Si Solar Cells", *Energy Procedia*, 2011, in press.

[14] B. Vermang et al, "On the Blistering of Atomic Layer Deposited Al_2O_3 as Si Surface Passivation", *Proc. 37th IEEE PVSC*, 2011, in press.

[15] A. Richter et al., "Firing Stable Al_2O_3/SiN_x Layer Stack Passivation for the Front Side Boron Emitter of n-type Silicon Solar Cells", *Proc. 25th EU PVSEC and 5th WC PEC*, 2010, pp. 1453-1459.

[16] F. Duerinckx et al., "Improved Screen Printing Process for Very Thin Multi-Crystalline Silicon Solar Cells", *Proc. 19th EU PVSEC*, 2004, pp. 443-446.